Rare Metal Materials and Engineering
Volume 50, Issue 8, August 2021
Available online at www.rmme.ac.cn

Science Press

Cite this article as: Qi Chunbao, Wang Tao, Wang Jintao, et al. Study on Adsorption Behavior of CO_2 on the δ-Pu(100) Surface Based on First-principles[J]. Rare Metal Materials and Engineering, 2021, 50(08): 2728-2737.

ARTICLE

Study on Adsorption Behavior of CO_2 on the δ-Pu(100) Surface Based on First-principles

Qi Chunbao[1], Wang Tao[2], Wang Jintao[2], Tao Sihao[1], Qin Ming'ao[1]

[1] Graduate School, Xi'an Institute of High-Tech, Xi'an 710025; China; [2] School of Nuclear Engineering, Xi'an Institute of High-Tech, Xi'an 710025; China

Abstract: A first-principles calculation was applied to study the adsorption behavior of CO_2 on δ-Pu(100) surface using a slab model within the framework of density functional theory. Results demonstrate that CO_2 molecules are adsorbed on δ-Pu(100) surface at C-terminated bent state by multi-bond binding of C-Pu and O-Pu. The adsorption type belongs to strong chemical adsorption and the most stable adsorption configuration is H_1-C_4O_4 with the adsorption energy of -6.430 eV. The adsorption stability order is hollow site> bridge site>top site. CO_2 molecule mainly interacts with Pu surface atoms, while the interaction with other three Pu atoms is weak. The transfer of more electrons to the CO_2 $2\pi_u$ orbital is beneficial to the bending and activation of C-O bonds. Moreover, the chemical bonding between Pu atoms and CO_2 molecule is mainly ionic state and the reaction mechanism is that the C 2s, C 2p, O 2s and O 2p orbitals of CO_2 molecule hybrid with Pu 6p, Pu 6d and Pu 5f orbitals, resulting in a new bond structure. The work function of the H_1-C_4O_4 site changes the least, indicating that other electrons readily escape from the metal surface and the required energy is the smallest.

Key words: plutonium surface; carbon dioxide; density functional theory; electron density; adsorption behavior; reaction mechanism

Plutonium, one of the most complicated elements in the periodic table, is at the boundary between the light actinide elements (Th to Pu) with itinerant 5f electrons and heavy actinide elements (Am and later elements) with localized 5f electrons. Elemental Pu and its alloys and compounds are widely used in the nuclear engineering, e. g., the nuclear devices, nuclear reactor and aerospace fields. In principle, the more localized 5f electrons in Pu-based materials[1,2] will produce many anomalous physical properties, such as the three-peak structures in the photoemission spectra (PES), the negative thermal expansion coefficient in Pu-Ga alloy and the abnormal magnetic properties, as compared to its neighboring element (U) in the periodic table. On the chemist's viewpoint, additionally, Pu is very active in the atmosphere environment, and easy to react with almost ordinary molecules in the ambient condition during purification, storage and usage of Pu-based materials. Energetically, PuO, Pu_2O_3 and PuO_2 are the basic products of plutonium oxidation[3-6], which pose a great challenge for the long-term storage and protection of plutonium-based materials. In fact, adsorption and dissociation behavior of the ordinary gaseous molecules on plutonium surface is essential processes for hydrogenation and oxidation corrosion. As a consequence, it is significant to study the adsorption and dissociation of active gases on the plutonium surface in order to deeply understand the corrosion and anti-corrosion mechanisms of Pu-based materials. As a matter of fact, scare direct experimental observation is conducted on Pu-based materials owing to their strong chemical activity, radioactivity and toxicity. For this reason, theoretical work might be an appropriate candidate for studying the adsorption and dissociation behavior of gas molecules on plutonium surface.

Eriksson et al[7] calculated the δ-Pu(100) surface under non-magnetic conditions by surface linear muffin-tin orbit method (FLMTO). The results showed that the 5f band is narrowed, the bonding ability decreases and the surface lattice constant is expanded. Huda et al[8-11] successively studied the adsorption behavior of hydrogen and oxygen atoms as well as hydrogen and oxygen molecules on the δ-Pu surface using density functional theory (DFT) and Dmol3 program, and results

Received date: August 13, 2020
Corresponding author: Wang Tao, Ph. D., Professor, School of Nuclear Engineering, Xi'an Institute of High-Tech, Xi'an 710025, P. R. China, E-mail: wtao009@163.com

showed that the 5f electron localization intensity of δ-Pu(111) surface is stronger than that of δ-Pu(100) surface. In addition, Li et al[12] studied the surface geometry and electronic structure of δ-Pu monolayer using the full potential linear conjugate plane wave method (FLAPW). The results indicated that δ-Pu (100) and (111) surface atoms show more localization features due to the decrease of the neighboring atom number and the overlap probability of 5f electron wave functions. As a result, the degree of localization of 5f electrons on (100) surface is stronger than on (111) surface, which is exactly opposite to Huda's results. Atta-Fynn et al[13,14] studied the adsorption of C, N, O atoms on δ-Pu(111) surface and the effect of surface relaxation on adsorption using FLAPW method. Meng et al[15] studied the adsorption and dissociation behavior of CO_2 molecule on Pu(100) surface using the modified Perdew-Burke-Emzerh (PBE) method based on the generalized gradient density functional theory and Dmol3 program. The calculated dissociation energy barrier of $CO_2 \rightarrow$ CO+O is 0.66 eV and the dissociation adsorption energy is 2.65 eV. Luo et al[16] studied the adsorption of CO molecule on Pu(100) surface by DFT and Dmol3 program. The results demonstrated that the dissociation energy barrier of CO molecules adsorbed on obliquely hollow is relatively small (0.280 eV). Wang et al[17] used GGA-DFT, Dmol3 and WIEN2k to study the adsorption of CO_2 on nano-layer of α-Pu (020) surface. The results revealed that the completely dissociated configuration (C+O+O) has the strongest surface binding energy (7.94 eV), followed by partial dissociated configuration (CO+O) and CO_2 molecular configuration (5.18 and 1.90 eV, respectively). Atta-Fynn et al[18] used ab initio calculation method within the framework of DFT and Dmol3 program to study the adsorption and dissociation behavior of CO_2 molecule on δ-Pu(111). The results indicated that the fully dissociated configuration (C+O+O) shows the strongest binding energy to the surface (7.92 eV), followed by the partially dissociated configuration CO+O (5.08 eV), with the lowest binding energy of CO_2 molecule adsorption (2.35 eV).

One can see that the theoretical researches on the surface properties and adsorption behavior of plutonium metal are still relatively few, and there are certain differences in the research results. Dmol3 program is mostly used in the research methods, so it is necessary to apply different methods to systematically study the above problems. At present, the theoretical calculation of CO_2 molecule adsorption on plutonium surface by VASP program has seldom been reported publicly. To the best of our knowledge, mechanically, δ-phase plutonium is more ductile and readily-processing than its other allotrope, such as the room temperature α phase. Therefore, we plan to perform a first principles calculation for the adsorption of CO_2 on a representative face of δ-phase plutonium, i.e., δ-Pu(100) surface. Specially, we focus on the stable adsorption configurations, the changes of electronic structure, the adsorption energies as well as the charge transfers induced by adsorption, which might give a new perspective on the corrosion and anti-corrosion mechanisms of CO_2 with δ-Pu(100) surface.

1 Computational Details

1.1 Methods

All calculations were implemented within Vienna ab-initio Simulation Package (VASP5.4.4)[19] on basis of density functional theory (DFT)[20,21]. It uses projection augmented wave (PAW)[22,23] pseudopotential method for first-principles calculation, which is an efficient plane wave pseudopotential package and widely used in the calculation of electronic structures[24,25]. Generalized gradient approximation (GGA) in the form of Perdew-Burke-Ernzerhof (PBE) exchange-correlation potential was used to approximate the electron exchange correlation interactions[26,27]. There are 16, 4 and 6 valence electrons in the outer shells for Pu ion ($6s^26p^65f^67s^2$), C ion ($2s^22p^4$) and O ion ($2s^22p^4$), respectively. Monkhorst-Pack (MP)[28] scheme was used to sample inside the irreducible Brillouin-zone. The spin polarization effect was considered in all calculations.

CO_2 molecule was packed in a box with side length of 1.5 nm when optimized, and the *k*-point mesh was set to 1×1×1. The ion position, cell shape and cell volume were changed when the δ-Pu cell was optimized with a 7×7×7 *k*-point mesh used. The lower two layers were fixed and the upper two layers were released for optimization with the shape and volume unchanged when the δ-Pu(100) 4-layer slab was optimized. We fixed the bottom 4, 3, and 2 layers, and released the CO_2 molecule, CO_2 and Pu surface atoms, CO_2 and upper two layers Pu atoms for optimizing, and the results showed that the geometrical parameters change little and the Pu atoms move slightly. In order to improve calculation efficiency and save calculation time, 4 layers of Pu atoms were fixed and CO_2 molecule on the optimized surface was released without changing its shape and volume when the CO_2 adsorption system on δ-Pu(100) 4-layer slab surface was optimized[15]. The *k*-point mesh of δ-Pu(100) surface and adsorption system were all set to 5×5×1. The proportional coefficient acting on force was 0.5 and N-order Methfessl-Paxton method was applied for the δ-Pu unit cell, whose surface and adsorption system were optimized. In all optimization calculations, a plane-wave cut-off energy of 450 eV was adopted to ensure the total energy of all structures converged within 0.5 MeV/atom, and the Conjugate Gradient (CG)[29] method of Hellman-Feynman force was applied for ion optimization. The convergence criterion of atomic force was 0.1 eV/nm and the energy convergence criterion was 10^{-4} eV. The total energy was acquired by one-step self-consistent calculation based on the optimized model. The charge density, work function and charge transfer of CO_2 molecule, δ-Pu(100) surface and adsorption system were also addressed in this study.

The surface energy, E_{sur}, is then obtained by Eq.(1):

$$E_{sur}=(E_{slab}-NE_{bulk})/2A \quad (1)$$

where A is the cross-sectional area of the slab, E_{slab} is the total energy of the slab, N is the number of Pu atoms in the slab and E_{bulk} is the energy of a single Pu atom in the bulk.

The adsorption energy of CO_2 molecule is given by

$$E_{ads}=E_{[CO_2/Pu(100)]}-E_{CO_2}-E_{Pu(100)} \quad (2)$$

where $E_{[CO_2/Pu(100)]}$ is the total energy of the system after adsorption, E_{CO_2} is the energy of the CO_2 molecular, $E_{Pu(100)}$ is the energy of the δ-Pu(100) surface before adsorption. The energy before and after adsorption is acquired under the same calculation method and accuracy. Furthermore, the energy of CO_2 is the basic state energy under the same calculation method. For negative adsorption energy, the structural stability is increased by adsorption. Moreover, the less the adsorption energy, the more stable the structure.

1.2 Models

1.2.1 δ-Pu and CO_2 models

The crystal structure of metallic δ-Pu is face centered cubic (fcc) with the space group code of Fm-3m, and the optimized Pu crystal lattice is 0.4772 nm, which is in good agreement with the experimental value of 0.4637 nm[9] at the error rate of 2.9%, as shown in Fig. 1. The optimized C-O bond length is 0.1177 nm, which is consistent with 0.1162 nm (in experiment) [30] at the error rate of 1.3% (as seen in Fig.2).

1.2.2 Surface and adsorption system models

From the test results of surface energy convergence and Ref. [15,16], we find that the E_{sur} difference of $p(3\times3)$ and $p(2\times3)$, $p(2\times3)$ and $p(2\times2)$ slabs is 0.7 and 4.3 eV·nm^{-2}, respectively. The differences are negligibly small and will not affect the main conclusion, so 4 layers of Pu atomic layer crystals (slab) of $p(2\times2)$ are established under the optimized δ-Pu unit cell to simulate the δ-Pu(100) surface. A vacuum layer with 1.5 nm thickness[31] is set on the z axis of the δ-Pu(100) surface to ensure that the interaction between adjacent layers is negligibly small. The lattice constant of the supercell is $a=b=$ 0.674 88 nm and c=2.215 81 nm, and slab model is shown in Fig.3a and Fig.3b, in which the z coordinate and layer spacing of the surface two Pu atoms decrease. Fig. 3c shows the adsorption sites on the δ-Pu(100) surface, where A represents bridge site, B represents hollow site, and C represents top site.

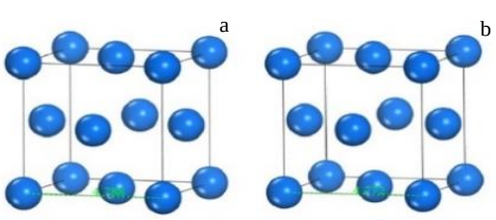

Fig.1 Crystal models of δ-Pu before (a) and after (b) optimization

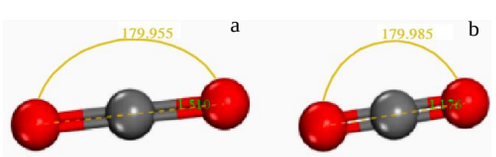

Fig.2 Crystal models of CO_2 molecule before (a) and after (b) optimization

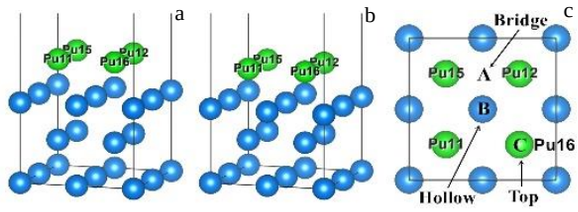

Fig.3 Structure model of δ-Pu(100) slab before (a) and after (b) optimization and top view of three adsorption sites on the surface (c) (surface Pu and other layers Pu atoms are in green and blue color, respectively)

Thus, there are three kinds of highly symmetrical adsorption sites. The adsorption model contains 16 Pu atoms and 1 CO_2 molecule with a total of 19 atoms when the CO_2 molecule is placed on the optimized slab model surface. What's more, the monolayer adsorption coverage (θ) of CO_2 is 0.25 monolayer (ML). For linear CO_2 molecule, each highly symmetric adsorption position can be divided into three situations due to its different positions: (1) the molecule is vertical to Pu surface (Ver), (2) the molecule is parallel to Pu surface but parallel to crystal axis (Hor1), and (3) the molecule is parallel to the Pu surface but parallel to the diagonal of the crystal axis (Hor2).

A total of 9 adsorption configurations are established, as shown in Fig.4.

2 Results and Discussion

2.1 Adsorption configuration and energy

Nine kinds of highly symmetric adsorption models are optimized, and it is found that the optimization under the vertical adsorption models does not converge, which means that CO_2 molecule in these models are not likely to adsorb on the δ-Pu(100) surface. For distinguishing, we define configurations in accordance with the adsorption position occupied by CO_2 and the number of bonds between CO_2 and Pu atoms adjacent to the surface layer. For instance, H_1-C_4O_4 means that CO_2 molecule is adsorbed on hollow parallel 1 and the C and O atoms are bonded to the adjacent 4 Pu atoms. As a result, six adsorption configurations are plotted in Fig. 5. The optimized structural parameters and adsorption energy of CO_2 adsorption configurations on δ-Pu(100) surface are shown in Table 1.

The value of adsorption energy and C-O bond length can be taken as the judgment of CO_2 adsorption strength for CO_2/metal adsorption system, i. e., the smaller the adsorption energy and the larger the C-O bond length, the greater the CO_2 adsorption strength and the more stable the adsorption.

According to Fig. 5 and the data in Table 1, and from the viewpoint of C-O bond length and the angle of $\theta_{O\text{-}C\text{-}O}$, the C-O bond length of adsorbed CO_2 molecule is 0.1222~0.141 81 nm, which is significantly larger than that of gaseous CO_2 molecule, indicating that the C-O bond is activated and weakened after CO_2 molecule is adsorbed. Based on the

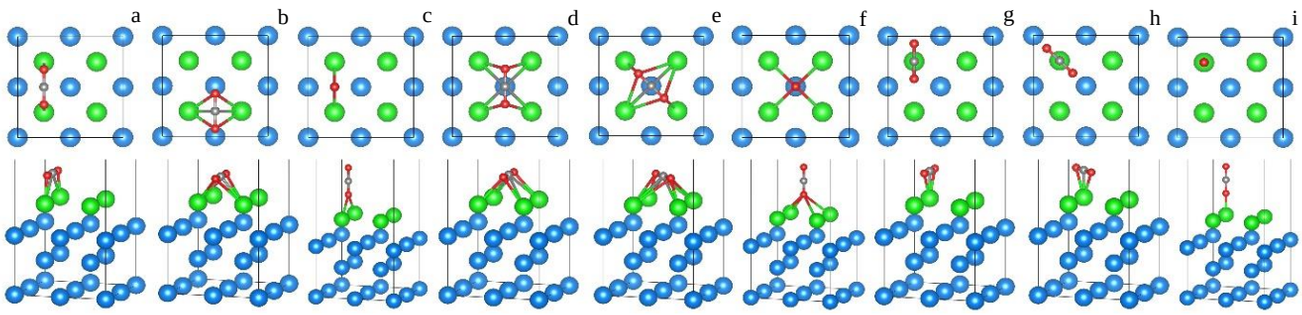

Fig. 4 Adsorption models of CO_2 on δ-Pu(100) surface: (a) bridge parallel 1, (b) bridge parallel 2, (c) bridge vertical, (d) hollow parallel 1, (e) hollow parallel 2, (f) hollow vertical, (g) top parallel 1, (h) top parallel 2 and (i) top vertical (C, O, surface Pu and other layers Pu atoms are in grey, red, green and blue colors, respectively)

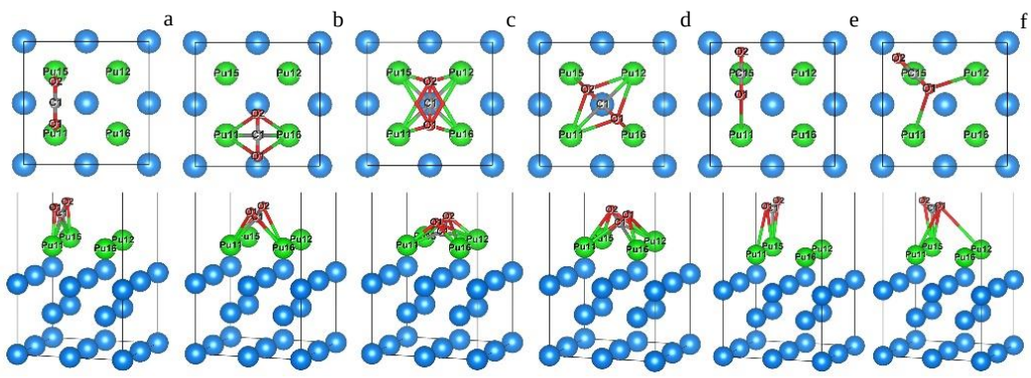

Fig.5 Top and side views of the optimized structures for CO_2 adsorption on δ-Pu(100) surface: (a) B_1-C_2O_2, (b) B_2-C_2O_2, (c) H_1-C_4O_4, (d) H_2-C_4O_3, (e) T_1-C_1O_2 and (f) T_2-C_1O_3 (B_1: bridge 1 site, B_2: bridge 2 site, H_1: hollow 1 site, H_2: hollow 2 site, T_1: top 1 site, T_2: top 2 site; C, O, surface Pu and other layers Pu atoms are in grey, red, green and blue color, respectively)

electron transfer of CO_2/δ-Pu(100) adsorption system, the activated CO_2 molecule after adsorption can be described as curved $CO_2^{\delta-}$ adsorption state, which is consistent with the general rule that $CO_2^{\delta-}$ is an important intermediate product of activated CO_2 adsorbed on metal[32], revealing that dissociation may occur in CO_2 molecule. The C-O bond length changes from B_1-C_2O_2 to T_2-C_1O_3 sites in sequence of 0.010 77, 0.009 40, 0.024 21, 0.012 80, 0.004 64 and 0.004 62 nm, indicating that the adsorption stability is hollow site>bridge site>top site. In all the optimized adsorption configurations, CO_2 molecule appear in-plane bending and the $\theta_{O\text{-}C\text{-}O}$ decreases from 180° to 114.80°~149.48°. Moreover, the H_1-C_4O_4 adsorption configuration has the largest C-O bond length (0.141 81 nm) and the smallest $\theta_{O\text{-}C\text{-}O}$ (114.80°), demonstrating that CO_2 adsorption strength is the largest under this adsorption site, i.e., the most stable configuration.

From the perspective of adsorption energy, except the adsorption energies of B_1-C_2O_2 and T_2-C_1O_3 configurations are positive, the adsorption energies of B_2-C_2O_2, H_1-C_4O_4, H_2-C_4O_3 and T_1-C_1O_2 adsorption configurations are -2.388, -6.430, -1.529 and -2.192 eV, respectively, which are significantly larger than 40 kJ/mol, showing that adsorption is strong chemical adsorption and the four adsorption configurations are stable. Furthermore, the order of adsorption stability is hollow site>bridge site>top site, which is consistent with the conclusion of C-O bond length analysis.

After adsorption, CO_2 molecule is adsorbed on δ-Pu(100) surface by multi-bond binding of C-Pu and O-Pu. The C-Pu bond length of C atom in CO_2 molecule and Pu surface atom is in the range of 0.242 52~0.274 12 nm, which approaches the C-Pu bond length in Pu carbide crystal (PuC: 0.246 20 nm, PuC_2: 0.228 19 nm) [33]. The O-Pu bond length between O atoms and the neighbor Pu surface atoms ranges from 0.226 70 nm to 0.234 76 nm, which is slightly larger than the O-Pu bond length (PuO: 0.1830 nm, PuO_2: 0.1810 nm)[34,35], indicating that CO_2 molecule is stably adsorbed on the δ-Pu(100) surface by strong bonding between C or O atoms and surface Pu atoms. From the bonding number and adsorption energy of B_2-C_2O_2, H_1-C_4O_4, H_2-C_4O_3 and T_1-C_1O_2 adsorption configurations, one can see that the more C-Pu and O-Pu bonds, the more stable the adsorption configuration.

From the height of C or O atoms away from Pu surface layer, $h_{C\text{-}S}$ in H_1-C_4O_4, H_2-C_4O_3, B_2-C_2O_2 and T_1-C_1O_2 adsorption configurations are 0.066 77, 0.134 93, 0.182 59 and 0.253 63 nm, respectively; $h_{O1(2)\text{-}S}$ are 0.143 17, 0.198 77, 0.233 62 and 0.285 81 nm, respectively. One can see that the smaller the $h_{C\text{-}S}$ and $h_{O1(2)\text{-}S}$, the lower the height of C or O atoms from Pu surface layer, and the more stable the

Table 1 Optimized geometrical and energy parameters of CO_2 adsorption on δ-Pu(100) surface

Configuration	$d_{C\text{-}O1(2)}$/×10^{-1} nm	Bond	$d_{C\text{-}Pu}$/×10^{-1} nm	Bond	$d_{O\text{-}Pu}$/×10^{-1} nm	$\theta_{O\text{-}C\text{-}O}$/(°)	$h_{C\text{-}S}$/×10^{-1} nm	$h_{O1(2)\text{-}S}$/×10^{-1} nm	E_{ads}/eV
B_1-C_2O_2	1.2837 (1.2837)	C-Pu11 C-Pu15	2.4252	O1-Pu11 O2-Pu15 O1-Pu15 O2-Pu15	2.3526 2.3526 3.6552 3.6552	129.21	1.7422	2.2927	4.896
B_2-C_2O_2	1.2700 (1.2700)	C-Pu11 C-Pu16	2.4861	O1-Pu11/16 O2-Pu11/16	3.1076 3.1076	132.62	1.8259	2.3362	-2.388
H_1-C_4O_4	1.4181 (1.4181)	C-Pu11/12 C-Pu15/16	2.4777 2.4777	O1-Pu11/16 O2-Pu12/15 O1-Pu12/15 O2-Pu11/16	2.2670 2.2670 3.6334 3.6334	114.80	0.6677	1.4317	-6.430
H_2-C_4O_3	1.3040 (1.3040)	C-Pu11/12 C-Pu15/16	2.7412 2.7412	O1-Pu16 O2-Pu15 O1-Pu11/12 O2-Pu11/12	2.3476 2.3476 3.3071 3.3071	121.37	1.3493	1.9877	-1.529
T_1-C_1O_2	1.2224 (1.2224)	C-Pu15	2.5363	O1/2-Pu15 O1-Pu11	3.0918 3.6037	149.48	2.5363	2.8581	-2.192
T_2-C_1O_3	1.2222 (1.2222)	C-Pu15	2.5792	O1/2-Pu15 O1-Pu11/12	3.1372 3.9510	148.80	2.5792	2.9079	5.671

Note: $d_{C\text{-}O1(2)}$ is the distance between the C and O atoms of CO_2 molecule; $d_{C\text{-}Pu}$ is the binding length between the adsorbed C or O and neighbor surface Pu atoms; $\theta_{O\text{-}C\text{-}O}$ is the O-C-O bond angle; $h_{C\text{-}S}$ or $h_{O1(2)\text{-}S}$ are the adsorption height of C or O with respect to the first layer; E_{ads} is the adsorption energy.

adsorption configuration. What's more, the stability order is hollow site>bridge site>top site, which has a good agreement with the previous analysis results.

2.2 Bader charge distribution

In principle, the atom loses electrons and the valence is positive when the corresponding net charge is negative. On the contrary, the atom gains electrons and the valence is negative when the corresponding net charge is positive. Charge transfer occurs between C/O and Pu atoms originating from CO_2 adsorption on the δ-Pu(100) surface. In order to clearly elucidate the interaction between CO_2 molecule and Pu surface atoms, Bader charge distribution[36] of CO_2/δ-Pu(100) adsorption system is calculated, as listed in Table 2. The $q_{substance}$ in Table 2 is defined as

$$q_{atom}=q_{Bader}-q_{valence} \quad (3)$$

where q_{atom}, q_{Bader} and $q_{valence}$ are the net charge, Bader charge and valence electron of atom, respectively. Fig. 6 shows the charging situation of ions in CO_2/δ-Pu(100) adsorption system.

As shown in Table 2, from the point of charge transfer, the adsorbed CO_2 molecule is in different charge states (within the range of 0.5365~2.0493 e). The q_{1st} changes remarkably from -0.4220 e to -1.007~-2.3739 e, while the q_{2nd} changes little from 0.5124 e to 0.4242~0.6128 e. The q_{3rd} changes slightly from 0.2700 e to 0.1162~0.2785 e, and the least change appears for q_{4th} case (from -0.3604 e to 0.2637~0.3910 e). All the above-mentioned results demonstrate that electrons are mainly transferred from the Pu surface atoms to CO_2 molecules, i. e., CO_2 molecule mainly interacts with the surface Pu atoms. However, the interaction with other three layers of Pu atoms is weak, which also indicates that it is reasonable to use 4 layers of Pu atomic layer crystals to simulate CO_2/δ-Pu(100) system.

When CO_2 are adsorbed to the hollow, bridge and top sites,

Table 2 Net charge distribution number of CO_2/δ-Pu(100) system (e)

Configuration	q_C	q_{O1}	q_{O2}	q_{total}	q_{1st}	q_{2nd}	q_{3rd}	q_{4th}
Atom	-1.9548	0.9686	0.9862	0.0000	-	-	-	-
free surface	-	-	-	-	-0.4220	0.5124	0.2700	-0.3604
B_1-C_2O_2	-0.9933	1.1052	1.1051	1.2170	-1.6652	0.5614	0.2442	-0.3572
B_2-C_2O_2	-1.1591	1.1152	1.1152	1.0714	-1.4623	0.6128	0.1162	-0.3382
H_1-C_4O_4	-0.0836	1.0664	1.0665	2.0493	-2.3739	0.4242	0.2383	-0.3379
H_2-C_4O_3	-0.9039	1.1220	1.1220	1.3401	-1.7176	0.4768	0.1644	-0.2637
T_1-C_1O_2	-1.5560	1.0693	1.0693	0.5829	-1.0553	0.6028	0.2577	-0.3882
T_2-C_1O_3	-1.6313	1.0839	1.0838	0.5365	-1.0070	0.5832	0.2785	-0.3910

Note: q_{1st}, q_{2nd}, q_{3rd}, and q_{4th} represent the total net charge number of the first to fourth layers on the surface of δ-Pu(100), respectively.

the bonding numbers between C atom and the Pu surface adjacent atoms are 4, 2 and 1, respectively, and the average charge carried by CO_2 molecules are 1.6947, 1.1442 and 0.5597 e, which show that the intensity of charge transfer from Pu atoms to CO_2 molecule is hollow site>bridge site>top site. Moreover, CO_2 molecule carries the most charge (2.0493 e) in H_1-C_4O_4 configuration, indicating that the adsorption configuration is the most stable, which is consistent with the conclusion drawn from the changes in the intensity of C-O bond length and the value of adsorption energy. It also proves that hollow site has more the advantage in electron transfer number and energy than the top site and bridge site, demonstrating that the more the bonding number between C atoms and Pu surface atoms, the more stable the adsorption configuration. At the same time, the adsorption of hollow site shortens the distance between the nearest Pu-O atoms compared to other adsorption sites, which is beneficial to the interaction between Pu and O atoms, i.e., the hollow site is more stable.

As can be seen from Fig. 6, C atoms lose electrons and are positively charged, O atoms gain electrons and are negatively charged, Pu atoms in the surface layer lose electrons and are positively charged, some Pu atoms in the subsurface layer get electrons and are negatively charged, and some Pu atoms in the bottom layer lose electrons and are positively charged after CO_2 adsorption, which is in good agreement with the analysis in Table 2. Fig. 7 shows the change of C-O bond length and $\theta_{O\text{-}C\text{-}O}$ with net charge in adsorbed CO_2 molecule. One can see that the C-O bond length increases approximately linearly with the increase of net charge, while the $\theta_{O\text{-}C\text{-}O}$ decreases approximately linearly with the increase of net charge, which shows that the activation and bending degree of C-O bond depends on the degree of electron transferred from Pu surface to CO_2 molecule, and more electrons transfer to CO_2 $2\pi_u$ orbit, which is beneficial to the bending and activation of C-O bond.

2.3 Electronic structure analysis

From the point of the microscopic mechanism, adsorption will result in the change of the electronic structure. For exploring the reaction mechanism between CO_2 molecule and Pu surface atoms, the binding character between the CO_2 molecule and Pu surface has been examined by the charge-density difference. For the fully relaxed, minimum total-energy configuration (H_1-C_4O_4), the charge-density difference is given by

$$\Delta\rho=\rho_{[CO_2/\delta\text{-Pu}(100)]}-\rho_{[\delta\text{-Pu}(100)]}-\rho_{(CO_2)} \quad (4)$$

where $\rho_{CO_2/\delta\text{-Pu}(100)]}$, $\rho_{[\delta\text{-Pu}(100)]}$ and $\rho_{(CO_2)}$ are charge densities of CO_2/δ-Pu(100) adsorption system, δ-Pu(100) surface and CO_2 molecule, respectively. The electronic density of states (DOS) of the most stable configuration (H_1-C_4O_4) is calculated. The isosurfaces of charge-density difference in this site are also addressed, as shown in Fig. 8. The spatial distribution of charge accumulation and loss is represented by contour lines in the charge-density difference, which can directly determine

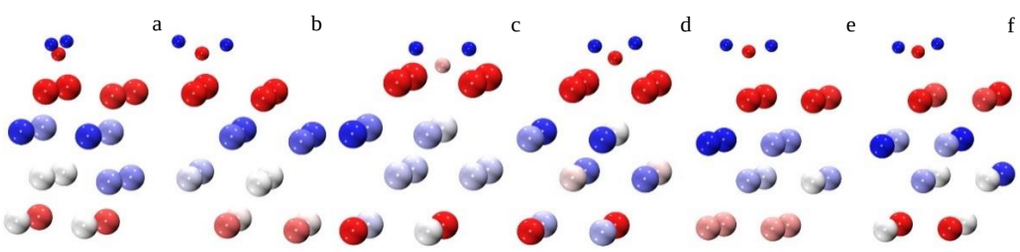

Fig.6 Charge state of each atom after CO_2 adsorption on δ-Pu(100) within the charge range of -0.20~0.20 e: (a) B_1-C_2O_2, (b) B_2-C_2O_2, (c) H_1-C_4O_4, (d) H_2-C_4O_3, (e) T_1-C_1O_2 and (f) T_2-C_1O_3 (red and blue mean positively and negatively charged, respectively)

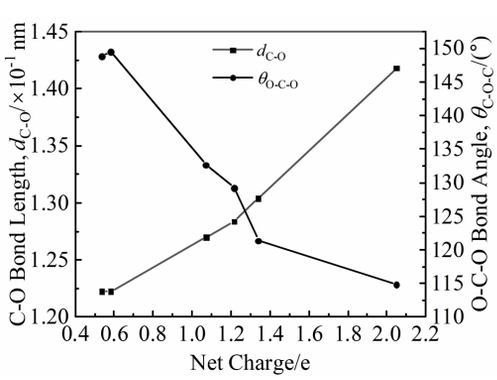

Fig.7 C-O bond length and O-C-O bond angle dependence of the net charges of chemisorbed CO_2

the bonding condition of ions in the adsorption system. Fig. 8 clearly shows that the CO_2 molecule gains electrons and the charge density increases obviously, while the Pu atoms in the surface layer lose electrons and the charge density decreases, which shows that there is no obvious spatial electron aggregation between the Pu atom and the CO_2 molecule, indicating that the chemical bonding between the Pu atom and C/O atoms is mainly ionic state.

In order to clearly demonstrate the chemical state in H_1-C_4O_4 configuration, we plot the 2D contour isosurfaces of the charge-density difference for Pu11, Pu12, Pu15 atoms and C1, O1, O2 atoms along the best planes of (001) and (010) in Fig. 9a and Fig. 9b, respectively. One can see that C/O atoms are surrounded by electrons, and there are no unpaired electrons between C/O and Pu atoms, demonstrating the ionic

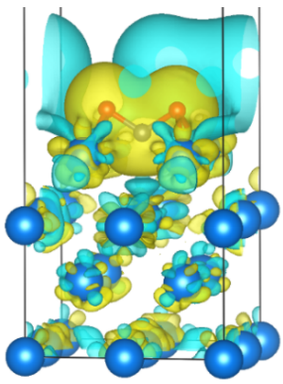

Fig.8 Isosurfaces of charge-density difference for the most stable configuration (H_1-C_4O_4) (yellow and blue color mean increase and decrease in charge density, respectively; isosurfaces level: 2 e/nm^3)

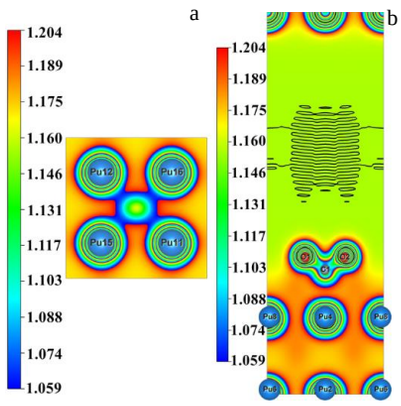

Fig.9 2D display of charge-density difference for H_1-C_4O_4 configuration: (a) plane of Pu11, Pu12, Pu15 atoms and (b) plane of C1, O1 and O2 atoms

chemical bond, which is in good agreement with the 3D isosurfaces of the charge-density difference in Fig.8.

Fig.10 shows the total density of states (TDOS) and partial density of states (PDOS) of clean δ-Pu(100) surface and TDOS and PDOS of the most stable adsorption configuration (H_1-C_4O_4) in the CO_2/δ-Pu(100) adsorption system. Fig. 11 shows the corresponding PDOS of H_1-C_4O_4 configuration. From Fig. 10a and 10b, one can see that the peak intensity, position and shape of TDOS on the δ-Pu(100) surface change remarkably induced from adsorption. The peak intensity increases in the range of -50 eV~ -45 eV. The peak shape broadens and the area becomes larger from -25 eV to -15 eV. Furthermore, the peak shape broadens obviously, the area increases and the peak value decreases in the range of -12.5~5 eV. Secondly, as shown in Fig.10c, 10d and Fig.11, the C 2s, C 2p and O 2s orbitals overlap and hybrid with Pu 6p orbital in the low energy level range of -25 eV~-15 eV, and the C 2s, C 2p, O 2s, O 2p orbitals overlap and hybrid with Pu 6d, Pu 5f orbitals in the high energy level (from -7.5 eV to 2.5 eV). The intensity of Pu 5f and Pu 6d peaks near E_F decreases slightly and the peak shape broadens, which indicates that the delocalization of Pu 5f and Pu 6d electrons becomes stronger and a small number of Pu 6d and Pu 5f electrons also participate in bonding. It is demonstrated that reaction

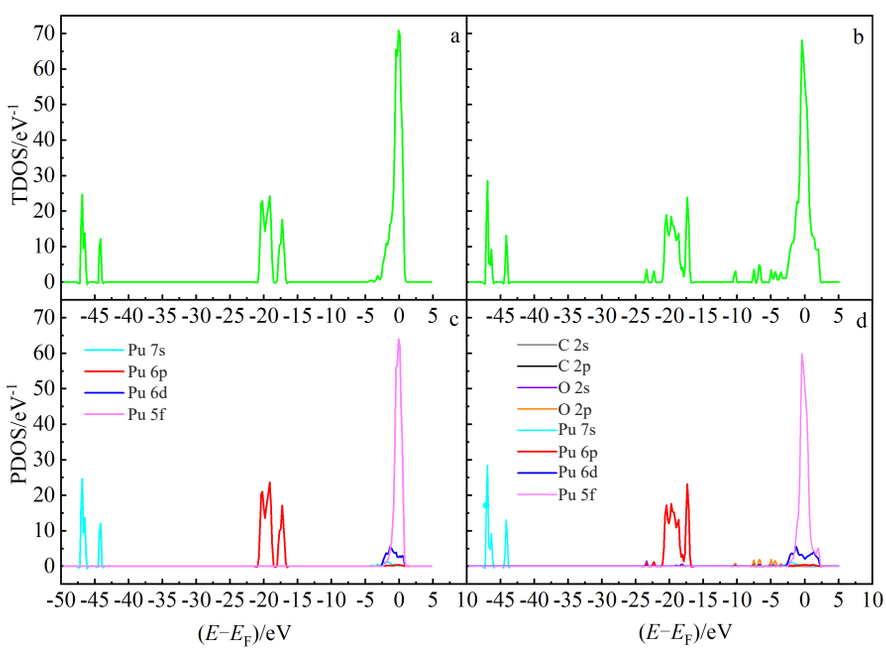

Fig.10 TDOS of clean δ-Pu (100) surface (a) and the most stable configuration (H_1-C_4O_4) (b); PDOS of clean δ-Pu (100) surface (c) and the most stable configuration (H_1-C_4O_4) (d)

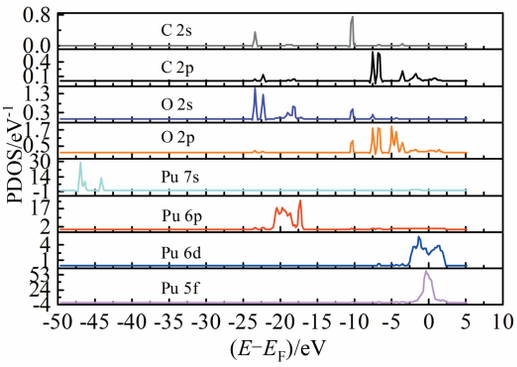

Fig.11 PDOS of the most stable configuration (H_1-C_4O_4)

mechanism between CO_2 molecule and surface Pu atoms is that the orbitals of CO_2 molecule hybrid with Pu 6p, Pu 6d and Pu 5f orbitals, resulting in a new chemical bonding state.

2.4 Surface work function analysis

Work function refers to the minimum energy that must be provided to enable an electron to escape from a solid surface immediately. It is the energy difference between the vacuum electrostatic potential and the Fermi level at infinity outside the metal, indicating the ability of electrons to escape from the metal surface. The calculation formula is as follows:

$$\Phi=E_{vacuum}-E_{Fermi} \quad (5)$$

where Φ, E_{vacuum} and E_{Fermi} are the work function, vacuum level and the Fermi level, respectively. The change of electrostatic potential along the distance to z-axis in all configurations is shown in Fig. 12, and the surface work function before and after adsorption is listed in Table 3.

At present, there is no experimental data of the work function of δ-Pu. The work function of its neighboring element (uranium) is in the range of 3.63~3.90 eV[37]. The work function of δ-Pu(100) exposed surface calculated by Wei et al is 4.365 eV [38], the work function of δ-Pu(111) slab calculated by Atta-Fynn et al is 3.39 eV[18], and the work function of δ-Pu(020) surface calculated under non-spin polarization condition is 3.53 eV[18]. In this work, the calculated work function of δ-Pu(100) surface is 2.9531 eV. The work function values of six sites increase at a certain extent in the range of 0.8644~1.8723 eV after adsorption. Moreover, the average change of the work function for hollow site is the smallest (1.0990 eV), for the top site is larger (1.4908 eV) and for the bridge site is the least (1.7812 eV). Among them, the work function change (0.8644 eV) of the H_1-C_4O_4 configuration is the smallest with the least adsorption energy (-6.430 eV), and meanwhile, the $h_{C\text{-}S}$ and $h_{O1(2)\text{-}S}$ are the lowest with the values of 0.066 77 and 0.143 17 nm, respectively, demonstrating that the energy is the lowest and the site is the most stable. For this reason, the energy of the system is the smallest, which indicates that other electrons readily escape from the metal surface and the required energy is the least.

2.5 Comparison with other researches

The calculation results in this work are compared with

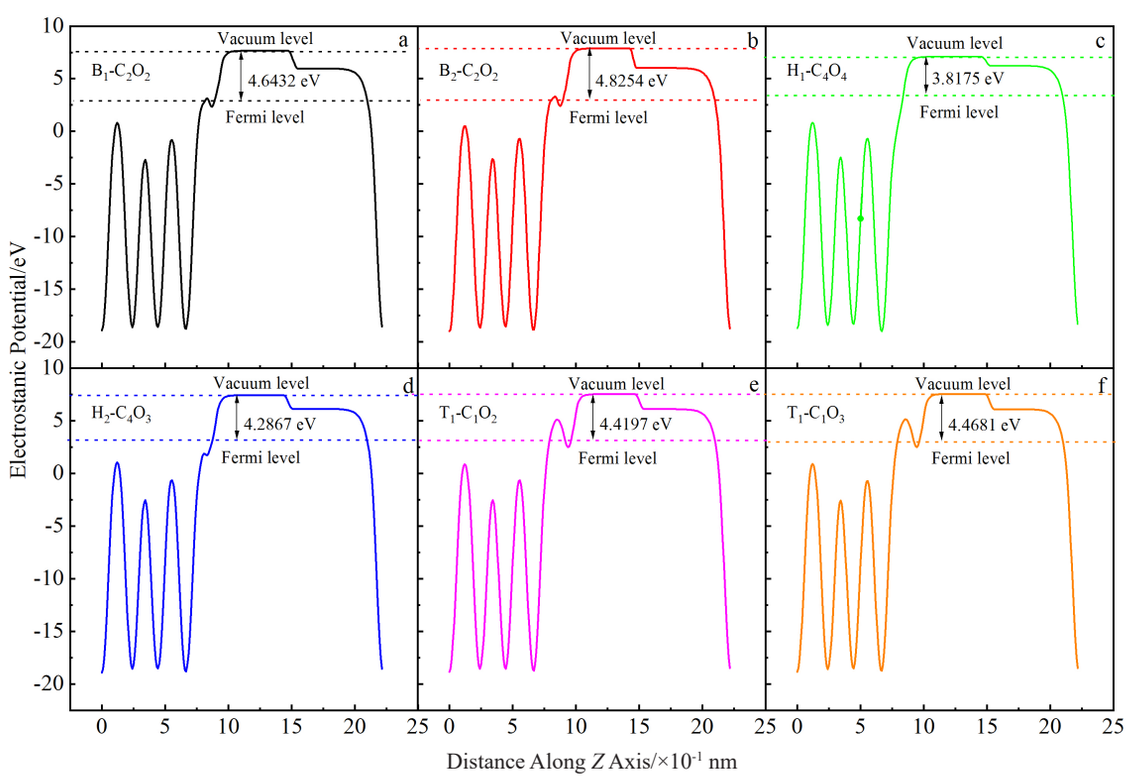

Fig.12 Change of electrostatic potential along distance to z-axis in all configurations: (a) ϕ=4.6432 eV, (b) ϕ=4.8254 eV, (c) ϕ=3.8154 eV, (d) ϕ=4.2867 eV, (e) ϕ=4.4197 eV, and (f) ϕ=4.4681 eV

Table 3 Surface work function changes of different adsorption configurations

Configuration	E_{vacuum}/eV	E_{Fermi}/eV	Φ/eV	$\Delta\Phi$/eV	$h_{C\text{-}S}$/×10^{-1} nm	$h_{O1(2)\text{-}S}$/×10^{-1} nm
Free surface	6.2523	3.2992	2.9531	-	-	-
B_1-C_2O_2	7.6613	3.0181	4.6432	1.6901	1.7422	2.2927
B_2-C_2O_2	7.8910	3.0656	4.8254	1.8723	1.8259	2.3362
H_1-C_4O_4	7.0719	3.2544	3.8175	0.8644	0.6677	1.4317
H_2-C_4O_3	7.4390	3.1523	4.2867	1.3336	1.3493	1.9877
T_1-C_1O_2	7.5370	3.1173	4.4197	1.4666	2.5363	2.8581
T_2-C_1O_3	7.5621	3.0940	4.4681	1.5150	2.5792	2.9079

Note: $\Delta\Phi$ means the change of the work function.

Table 4 Comparison of adsorption results of CO_2 molecule on Pu surface

Substance	Surface	Optimal configuration	$d_{C\text{-}O}$/nm	q/e	E_{ads}/eV	Φ/eV	Program	Functional	Pseudopotential
CO_2	δ-Pu(100)	H_1-C_4O_4	0.1418	2.05	-6.43	3.82	VASP	GGA-PBE	PAW
CO_2 [15]	δ-Pu(100)	Center vertical	0.1373	-0.79	1.48	-	DMOL3	DNP	DSPP
CO_2 [17]	α-Pu(020)	Long bridge	0.1280	-	1.46	3.53	DMOL3	DNP	DSPP
CO_2 [18]	δ-Pu(111)	Hor1 t1	0.1350	-	1.69	3.39	DMOL3	DNP	DSPP

Note: $d_{C\text{-}O}$ is the distance between the C and O atoms in CO_2 molecule; q is the transfer charge between CO_2 molecule and Pu atoms; E_{ads} is the adsorption energy; Φ is the work function of the Pu surface.

those in other references, as shown in Table 4.

From Table 4, one can see that the adsorptions of CO_2 molecule on Pu surface are all chemical adsorption from the absolute value of the adsorption energy. Most of the optimal adsorption configurations are center or hollow sites and one is bridge site. The absolute values of adsorption energy, work function and $d_{C\text{-}O}$ calculated are the largest in this work. The reasons may be that we use different programs and methods, Dmol3 uses DSPP basic, belonging to quantum chemistry method, while VASP uses PAW pseudopotential, belonging to density functional method, which may lead to various results; however, these results belong to the same numerical magnitude, and most importantly, the calculated adsorption energies are relatively different, so we can distinguish which site is the most favorite. Furthermore, the quantitative values have slight effect on the conclusion originated from qualitative analysis.

3 Conclusions

1) CO_2 molecule are adsorbed on the δ-Pu(100) surface by multi-bonds binding of C-Pu and O-Pu. The adsorption type belongs to strong chemical adsorption. Furthermore, the most stable adsorption configuration is H_1-C_4O_4 with the adsorption energy of -6.430 eV, and at this time, the C-O bond length is 0.141 81 nm and $\theta_{O\text{-}C\text{-}O}$ is 114.80°. The order of adsorption stability is hollow site>bridge site>top site, and the more the bond number of C-Pu and O-Pu, the lower the height of C or O atom from Pu surface layer, the more stable the configuration.

2) The adsorbed CO_2 molecule are charged to different degrees (0.5365~2.0493 e) and CO_2 molecules carry the most charge (2.0493 e) for H_1-C_4O_4 configuration. CO_2 molecule mainly interacts with the surface Pu atoms. The transferring intensity of charge from Pu atoms to CO_2 molecule is hollow site>bridge site>top site, which is consistent with the conclusion of angle analysis of C-O bond length and adsorption energy. The chemical bonding between Pu atoms and C/O atom is mainly ionic state and the reaction mechanism between CO_2 molecule and surface Pu atoms is that the C 2s, C 2p, O 2s and O 2p orbitals of CO_2 molecule hybrid with Pu 6p, Pu 6d and Pu5f orbitals to produce new chemical bonding state.

3) The work function of the six configuration increases in the range of 0.8644~1.8723 eV after CO_2 adsorption, and the work function of the H_1-C_4O_4 site changes the least. Furthermore, the energy of the system is the smallest, which indicates that other electrons readily escape from the metal surface and the required energy is the least.

References

1 Haschke J M, Hodges A E, Lucas R L. *Journal of the Less Common Metals*[J], 1987, 133(1): 155

2 Méot-Reymond S, Fournier J M. *Journal of Alloys & Compounds*[J], 1996, 232(1-2): 119

3 Almeida T, Cox L E, Ward J W *et al*. *Surface Science Letters*[J], 1993, 287(1): 141

4 Stakebake J L, Larson D T, Haschke J M. *Journal of Alloys and Compounds*[J], 1993, 202(1): 251

5 Oetting F L. *Chemical Reviews*[J], 1967, 67(3): 261

6 Haschke J M, Ricketts T E. *Journal of Alloys & Compounds*[J], 1997, 252(1-2): 148

7 Eriksson O, Hao Y G, Cooper B R *et al*. *Physical Review B Condensed Matter*[J], 1991, 43(6): 4590

8 Huda M N, Ray A K. *Physica B Physics of Condensed Matter*[J], 2005, 366(1-4): 95

9 Huda M N, Ray A K. *The European Physical Journal B*[J], 2004, 40(3): 337

10 Huda M N, Ray A K. *The European Physical Journal B*[J], 2005, 43(1): 131

11 Huda M N, Ray A K. *Physica B-Condensed Matter*[J], 2004, 352: 5

12 Li G, Lai X C, Sun Y. *Acta Physico-Chimica Sinica*[J], 2005, 21(6): 686 (in Chinese)

13 Atta-Fynn R, Ray A K. *Physical Review B*[J], 2007, 75(19): 5112

14 Atta-Fynn R, Ray A K. *Physica B Physics of Condensed Matter* [J], 2007, 400(1-2): 307

15 Meng Daqiao, Luo Wenhua, Li Gan *et al*. *Acta Physica Sinica* [J], 2009, 58(12): 8224 (in Chinese)

16 Luo Wenhua, Meng Daqiao, Li Gan *et al*. *Acta Physica Sinica* [J], 2008, 57(1): 160 (in Chinese)

17 Wang Jiangguang, Aosk K. *Journal of Computational and Theoretical Nanoscience*[J], 2014, 11: 1710

18 Atta-Fynn R, Ray A K. *European Physical Journal b Condensed Matter & Complex Systems*[J], 2009, 70(2): 171

19 Kresse G, Furthmüller J. *Physica B Physics of Condensed Matter* [J], 1996, 54(16): 111 69

20 Hohenberg P, Kohn W. *Physical Review*[J], 1964, 136: 864

21 Kohn W, Ham L J. *Physical Review A*[J], 1965, 140: 1133

22 Blochl P E. *Physica B Physics of Condensed Matter*[J], 1994, 50: 17 953

23 Kresse G, Joubert D. *Physical Review B*[J], 1999, 59(3): 1758

24 Huang G Y, Wang C Y, Wang J T. *Journal of Physics-Condensed Matter*[J], 2009, 21: 345 802

25 Dong W, Kresse G, Furthmüller J *et al*. *Physica B Physics of Condensed Matter*[J], 1996, 54(3): 2157

26 Perdew J P, Chevary J A, Vosko S H *et al*. *Physical Review*[J], 1992, 46: 6671

27 Perdew J P, Burke K, Ernzerhof M. *Physical Review Letter*[J], 1996, 77: 3865

28 Monkhorst H J, Pack J D. *Physical Review B Condensed Matter* [J], 1976, 13: 5188

29 Payne M C, Arias T A, Joannopoulos J D. *Reviews of Modern Physics*[J], 1992, 64(4): 1045

30 Ogren, Paul J. *Journal of Chemical Education*[J], 2002, 79(1): 117

31 Li Gan, Luo Wenhua, Chen Huchi. *Acta Physico-Chimica Sinica* [J], 2011, 27(10): 2319 (in Chinese)

32 Freund H J, Messmer R P. *Surface Science*[J], 1986, 172(1): 1

33 Li Gan, Sun Ying, Wang Xiaolin *et al*. *Acta Physico-Chimica Sinica*[J], 2003, 4: 356 (in Chinese)

34 Green D W, Reedy G T. *Chemischer Informationsdienst*[J], 1978, 69(2): 544

35 Haire R G. *Journal of Alloys & Compounds*[J], 1994, 213-214: 185

36 Henkelman G, Amaldsson A, Jonsson H. *Computational Materials Science*[J], 2006, 36: 354

37 Hao Y G, Eriksson O, Fernando G W *et al. Physica B Physics of Condensed Matter*[J], 1993, 47(11): 6680

38 Wei Hongyuan, Hu Rui, Xiong Xiaoling *et al*. *Journal of Molecular Science*[J], 2010, 26(1): 37 (in Chinese)

CO_2在δ-Pu(100)表面吸附行为的第一性原理研究

戚春保[1]，王　涛[2]，王金涛[2]，陶思昊[1]，秦铭澳[1]

(1. 火箭军工程大学 研究生院，陕西 西安 710025)

(2. 火箭军工程大学 核工程学院，陕西 西安 710025)

摘　要：结合密度泛函理论框架内的周期性平板模型，运用第一性原理计算方法研究了CO_2在δ-Pu(100)表面的吸附行为。结果表明，CO_2分子以C端向下和C-Pu、O-Pu多键结合的方式吸附在δ-Pu(100)表面。吸附类型属于强化学吸附，最稳定的吸附构型是H_1-C_4O_4，此时吸附能为-6.430 eV，吸附稳定性顺序为穴位>桥位>顶位。CO_2分子主要和表面Pu原子反应，而与其它3层Pu原子的反应较弱。更多的电子向CO_2 $2\pi_u$轨道转移有利于C-O键的弯曲和活化。此外，CO_2分子和Pu原子之间的化学键主要是离子态，反应机理是CO_2的C 2s、C 2p、O 2s和O 2p轨道与Pu 6p、Pu 6d、Pu 5f轨道发生了重叠杂化作用，产生了新的键结构。H_1-C_4O_4构型的功函数变化最小，表明其它电子容易从该构型表面逃逸，且需要的能量最小。

关键词：钚表面；CO_2；密度泛函；电子密度；吸附行为；作用机理

作者简介：戚春保，男，1995年生，硕士生，火箭军工程大学研究生院，陕西 西安 710025，E-mail：za7966093@qq.com